

# Observation of thermal microwave photons with a Josephson junction detector

A. L. Pankratov,<sup>\*</sup> A. V. Gordeeva,<sup>†</sup> A. V. Chiginev, L. S. Revin, and A. V. Blagodatkin  
*Nizhny Novgorod State Technical University n.a. R. E. Alekseev, Nizhny Novgorod 603950, Russia and  
Institute for Physics of Microstructures of RAS, Nizhny Novgorod 603950, Russia*

N. Crescini  
*Fondazione Bruno Kessler (FBK), I-38123, Trento, Italy and  
Univ. Grenoble Alpes, CNRS, Grenoble INP, Institut Néel, 38000 Grenoble, France*

L. S. Kuzmin  
*Nizhny Novgorod State Technical University n.a. R. E. Alekseev, Nizhny Novgorod 603950, Russia and  
Chalmers University of Technology, 41296 Gothenburg, Sweden*  
(Dated: April 17, 2024)

When measuring electromagnetic radiation of frequency  $f$ , the most sensitive detector is the one that counts the single quanta of energy  $hf$ . Single photon detectors (SPDs) were demonstrated from  $\gamma$ -rays to infrared wavelengths [1–3], and extending this range down to the microwaves is the focus of intense research [4–10]. The energy of 10 GHz microwave photon, about  $40 \mu\text{eV}$  or  $7 \text{yJ}$ , is enough to force a superconducting Josephson junction into its resistive state, making it suitable to be used as a sensor [11–17]. In this work, we use an underdamped Josephson junction to detect single thermal photons stochastically emitted by a microwave copper cavity at millikelvin temperatures. After characterizing the source and detector, we vary the temperature of the resonant cavity and measure the increased photon rate. The device shows an efficiency up to 40% and a dark count rate of 0.1 Hz in a bandwidth of several GHz. To confirm the thermal nature of the emitted photons we verify their super-Poissonian statistics [18, 19], which is also a signature of quantum chaos [20, 21]. We discuss detector application in the scope of Dark Matter Axion searches [22], and note its importance for quantum information [23–26], metrology [27, 28] and fundamental physics [15, 29].

The emission of black body radiation and photoelectrons were respectively explained by Planck and Einstein with the quantisation of the electromagnetic field [30]. Photons, the resulting quanta of light, are massless particles whose energy  $E$  is related to their frequency  $f$  by the Planck’s constant  $h$  through the relation  $E = hf$ . The most energetic photons ever recorded have  $E > 100 \text{TeV}$  [31] and belong to the class of gamma rays, which extends down to  $E \sim \text{MeV}$ . Lower energy photons are known as X-rays and have  $E \sim \text{keV}$ . Single photons in the gamma and X-ray range are detected with techniques belonging to the world of high-energy physics, for example crystal scintillators and photomultiplier tubes [32]. In the optical domain, a photon typically has an energy  $E \sim \text{eV}$ , and single photons can be detected by established means, for instance photomultipliers (tubes or solid state) or avalanche photodiodes [33]. The use of superconductors pushed the detectable energy down to the infrared range, with  $E \sim \text{meV}$ , by using nanowires [34, 35], transition-edge sensors [36], kinetic inductance detectors [3] and Josephson junctions (JJ) [2]. The microwave range, with  $E \sim 40 \mu\text{eV}$  ( $\sim 7 \text{yJ}$ ), is the frontier of single photon detectors [37], approached by quantum dots [4] and bolometric schemes [38–40]. The detection of single microwave photons attracted the attention of quantum technologies, and several circuit quantum electrodynamics schemes [41] were proposed [26, 42] and implemented using superconducting resonators and qubits [5–10, 43, 44].

The need of a microwave single photon detector (SPD) is witnessed by the field of Dark Matter particle searches, such as axions [45, 46]. In particular, Dark Matter haloscopes [47–50] rely on precision power measurements using low noise amplifiers, and the upgrade to photon detectors is utmost important [22, 51], since it outperforms quantum limited amplifiers or quantum enhanced measurements [22, 52]. Especially at higher frequencies, i. e. above a few GHz, the standard quantum limit of linear amplification [22, 53] drastically hinders the sensitivity of these measurements. The discovery of axions is a compelling argument, but the requirements needed for their detection are rather strict. The axionic signal is a stochastic emission of rare photons of frequency  $f_a$ , dependent on the unknown axion mass, in a narrow bandwidth  $10^{-6} f_a$  [45]. Therefore, a suitable photon detector should have a low dark count rate, wide spectral range, high efficiency, and be capable of continuous operation. Except for a few schemes circumventing some of these issues [9, 44], these conditions are typically not fulfilled by existing microwave photon detectors, and only some recent experiments [43, 54], could tackle the issue. The use of Josephson junctions as threshold detectors was proposed and analyzed in [15], but realised for detecting high photon rates only [17], while a detector of rare photons still poses an experimental challenge.

In this work, we demonstrate the detection of microwave single photons with high efficiency and sub-hertz dark count rate by using an underdamped Josephson

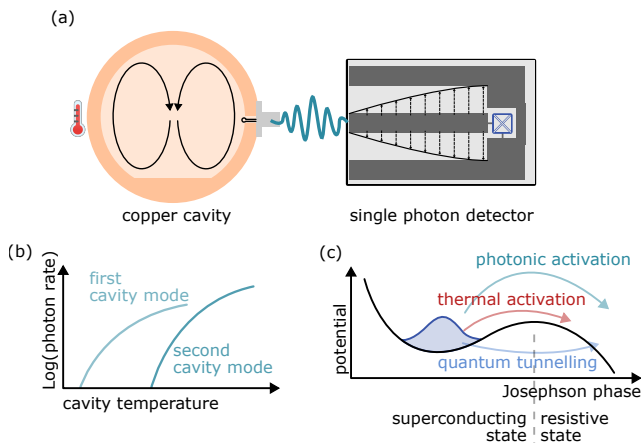


FIG. 1. Description of the experimental scheme. a) A microwave cavity is connected to the photon detector, where the former acts as a source of thermal photons and the latter is formed by the Josephson junction, inserted into a coplanar waveguide adapter. b) Temperature dependence of the thermal photons emitted by the cavity, whose exponential trend is used to vary the photon rate by orders of magnitude with a corresponding temperature change of tens of millikelvin. c) The tilted washboard potential describes the dynamics of a Josephson junction: the system is superconducting if the wavefunction is confined to a minimum, and resistive if it runs down the potential. The switching to the resistive state can be due to the signal, i.e. the arrival of a photon, or to noise, configured as thermal escape or quantum tunnelling processes, which therefore needs to be suppressed. See text for further details.

junction. The photons are generated by the thermal emission of a bulk microwave resonator made of copper. The experimental scheme and principles of operation are shown in Fig. 1. We engineer an experiment where the cavity design defines the frequency of the emitted photons, the rate of emission is adjusted from less than one photon per hour to thousands photons per second by varying the cavity temperature, and the photons are collected in the detector with an on-chip impedance matching line terminated by a JJ. When impinged by a photon, the current-biased junction switches to the resistive state making the detector click. The observed thermal photons depend exponentially on temperature and, when sourced from a single mode, follow a super-Poissonian statistics [18, 19], a unique signature of their nature.

The experiment is essentially composed of two parts: a photon source and a photon detector, shown in Fig. 2. The photon source of this experiment is a cylindrical cavity with the radius and length of about 3.0 cm and 1.2 cm, respectively, see Fig. 2a. The body is oxygen-free high conductivity copper to ensure a proper thermalization and a quality factor of the order of  $10^4$ . The cavity is coupled to two SMA outputs (port 1, weakly coupled, and port 2, close to critically coupled) through two loop antennas. The measured  $S_{21}$  transmission of the resonator

is reported in Fig. 2b, and shows the first four resonant modes. The detector is an underdamped Al-AlO<sub>x</sub>-Al Josephson junction directly connected to the cavity antenna and, upon the arrival of a photon, switches to the running state, producing a measurable voltage drop of hundreds of microvolts. The chip layout, the optical and scanning electron microscope (SEM) images of the coplanar line and Josephson junction are presented in Fig. 2c, while the switching rate of the detector for several cavity temperatures is reported in Fig. 2d. The on-chip coplanar line is designed as an impedance transformer from 50 to 200 Ohm, but the matching efficiency is sufficiently high (i.e. above 60%) even for junctions with  $R_N$  up to 2 kΩ as shown by numerical simulations. The microwave cavity port 2 feeds the signal via a short coaxial cable, soldered to the PCB coplanar line, which is further bonded to the coplanar line of the chip. The T-filters for the bias and voltage lines are composed of feed-through capacitances (1.1 nF, red), on-plate resistors (500 Ohm, blue) and larger resistors outside the sample holder (10 kOhm, not shown). The SPD is located inside cryoperm and superconducting screens to minimise the magnetic noise and residual stray light, as shown in the Methods.

The SPD is fabricated by shadow evaporation technique as Al-AlO<sub>x</sub>-Al trilayer on a Si substrate, its area is  $2.5 \times 0.7 \mu\text{m}^2$ , the measured critical current at 17 mK is  $I_C = 170 \text{ nA}$ , and the normal state resistance is  $R_N = 1480 \Omega$ . The choice of the junction parameters is targeted to a reduced dark count rate and optimal quantum efficiency. The former requires a reduction of thermal activation and quantum tunneling events [15], while the latter is related to the junction critical current and damping. For the latter, one needs to use an underdamped junction to avoid phase retrapping in the washboard potential, which effectively turns the junction back to the superconducting state, hindering the measurements of switching events. The sample presented hereafter has a critical current close to the optimal value for photon counting experiments [15], and was therefore chosen among others, which were still capable of detecting single photons but with slightly worse performances.

An underdamped Josephson tunnel junction is well-known as a detector of a harmonic signal with a minimum detectable power down to femtowatts level, by measuring the photon-assisted tunneling (PAT) steps at the inverse branch of a current-voltage characteristic. In this work we use PAT steps to measure resonant curves of the cavity at low temperatures, as detailed in the Methods, to then demonstrate that the Josephson junction also works as a microwave single photon detector when its bias current  $I$  is slightly lower than the critical current  $I_C$ . As outlined in Fig. 1, the dynamics of a Josephson junction can be treated as evolution of a phase particle in a tilted washboard potential. An absorbed photon causes a current pulse  $\Delta I$  through the junction, overcoming the threshold, and thus leading to the appearance of

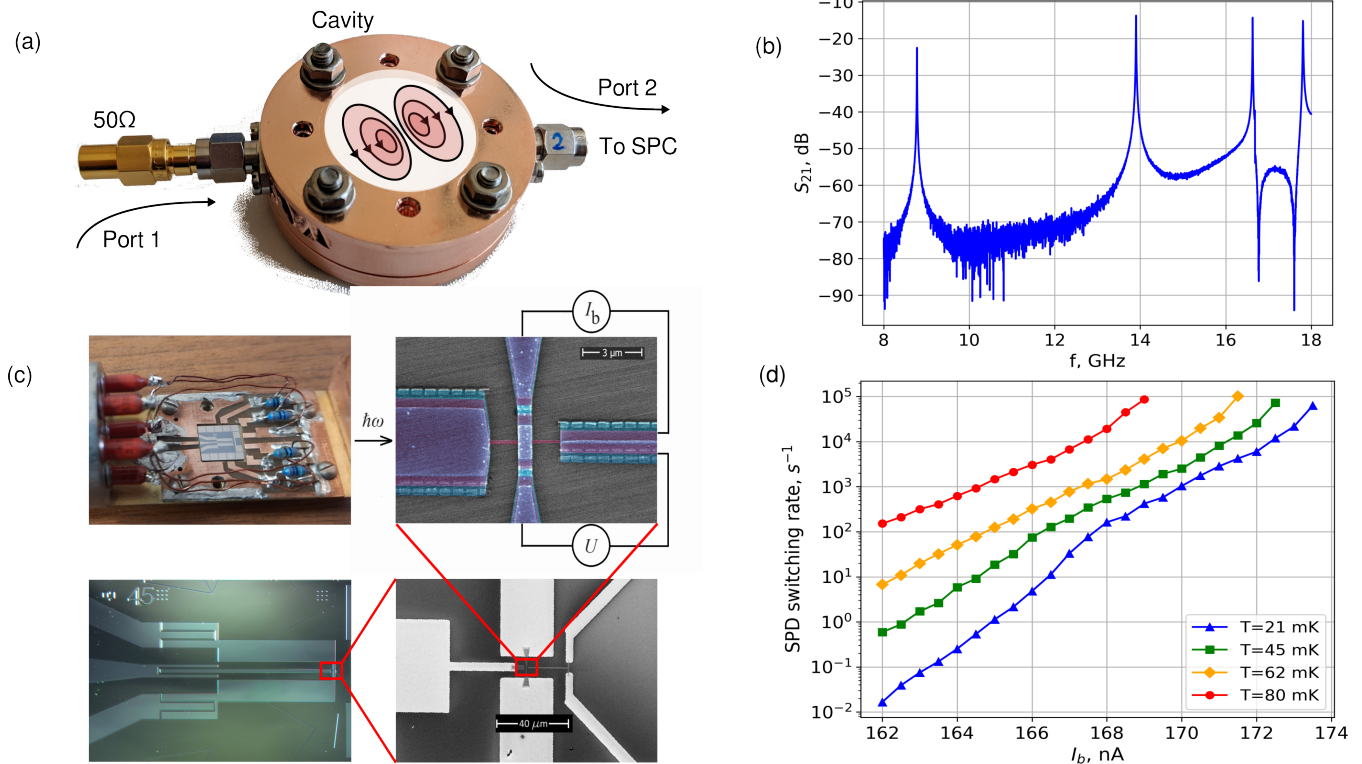


FIG. 2. Microwave cavity and photon detector used in this work. a) The cavity, critically coupled to the SPD through antenna port 2, while port 1 is very weakly coupled (used for characterisation purposes). At the centre of the cavity, a sketch of the 14 GHz mode shape is shown. b) The room temperature response of the cavity shows the resonant modes starting from the lower frequency mode at 8.81 GHz. The comparison with resonances at 17 mK are shown in Methods. c) Optical and SEM images of the detector directly connected to the cavity antenna. Top left: sample mounted in the sample holder. Bottom left: optical image of the chip. Top right: SEM of the Josephson junction with artificial colors. Pink - bottom Al electrode, blue - top Al electrode, violet - overlapping areas. Bottom right: the end of the coplanar line connected to the Josephson junction. The feeding d.c. lines are also shown bias current  $I_b$  and measured voltage  $U$ . d) The switching rates of the detector, measured at the base temperature 17 mK, for various cavity temperatures from 21 to 80 mK.

a measurable resistive state [15] with a finite voltage of about 0.4 mV. In the Josephson circuit, the energy  $hf$  of the incoming photon is split between the energy of the supercurrent  $E_s$  stored in the tank circuit and the energy  $E_d$  dissipated in the subgap resistor  $R_{qp}$ , approaching  $R_N$  close to zero voltage, according to quasiparticle IV curve of a tunnel Josephson junction [55]. Assuming the simple relation between  $E_s$  and the pulse amplitude  $\Delta I$  [15],  $E_s = L_{JJ}\Delta I^2/2$ , and taking into account that in parallel RLC-resonant circuit  $Q = R_N(C/L_{JJ})^{1/2}$ ,  $E_s/E_d = Q/2\pi$ , the current increase due to the photon can be estimated as  $\Delta I = \sqrt{2hfL_{JJ}^{-1}(1 + 2\pi/Q)^{-1}}$ , where the junction inductance  $L_{JJ}$  depends on the bias current  $I$  as  $L_{JJ} = \hbar/(2e)(I_C^2 - I^2)^{-1/2}$ . Using the above parameters, the single photon current pulse  $\Delta I$  is estimated to be about 60 nA.

The average number of thermal photons in a cavity mode follows the Planck distribution and depends on the modes' resonance frequency, loaded quality factor, and

temperature. Dissipation regulates the photon lifetime, giving rise to an emission rate that can be controlled by coupling an antenna to the mode [56]. On first approximation, the cavity photon rate  $r_c(T)$  measured with a SPD can be calculated considering  $n$  modes as

$$r_c(T) = \sum_{i=1}^n \frac{\eta_i}{\tau_i} \frac{1}{e^{hf_i/k_B T} - 1} \quad (1)$$

where  $f_i$ ,  $\tau_i$  are the frequencies and the lifetimes of the cavity modes' photons, respectively;  $h$  is the Planck constant,  $k_B$  is the Boltzmann constant and  $T$  is the temperature. The photon lifetime  $\tau_i = Q_i/(2\pi f_i)$  is extracted from the quality factor  $Q_i$  of the mode and its central frequency  $f_i$ . The parameters  $\eta_i$  are the ratio between the thermally available photons and the detected ones, it depends on the cavity antenna coupling and on the detector quantum efficiency. Thanks to the exponential dependence of the rate on the  $hf_i/k_B T$  ratio, at low enough temperatures only a limited number of modes significantly contribute to the rate, allowing us to neglect

the effect of higher order resonances.

After a preliminary room-temperature spectroscopic characterization, the cavity was mounted on the mixing chamber plate of a dilution refrigerator, and connected to the SPD. The cavity spectroscopy was repeated at 17 mK by sending a microwave tone to the cavity via port 1 and observing the first three cavity resonances as PAT steps in the current-voltage characteristic of the junction [17, 57]. The results of these measurements are shown in Methods.

In Fig. 2d, the SPD is characterised by measuring its mean switching rate versus a bias current for various cavity temperatures. To this end, the temperature of the cold plate of a dilution fridge was fixed at about 17 mK, while the cavity, only weakly thermally coupled to the plate, was heated by a resistor to a temperature of 21 to 80 mK, precisely controlled using a SQUID noise thermometer. The mean switching rate coincides with the SPD dark count rate at the lowest cavity temperature of 21 mK in absence of thermal photons, while it is defined by the photon rate at a large cavity temperature. One can see that the switching rate, starting from 0.01 Hz at the smallest bias current, increases by four orders of magnitude when heating cavity up to 80 mK, demonstrating the efficient response to incoming photons. It was checked that the switching rate nearly does not change at the same cavity temperature variation if the sample is disconnected from the cavity, and also that the response is heavily suppressed if the cavity is connected to the SPD by the port 1.

To observe the variation of the photon rate and characterise the quantum efficiency and dark count rate of the detector, we measured the temperature dependence of the switching events. In Fig. 3a we present an event plot of the recorded data at various temperatures, from 21 to 62 mK, showing an exponential increase of the switching rate. Fig. 3b displays the photon rate vs temperature and its fit. We fit the data with the expected cavity photon rate  $r_c(T)$  in Eq. (1) plus a dark count rate  $r_{DC} = 1/\tau_0$ , which is the inverse of the mean switching time  $\tau_0$  taken from the lowest temperature data, to extract the efficiency and noise floor of the detector. For this analysis, the quality factors and resonance frequencies are fixed to the values measured using PAT steps, see Methods. In particular, at  $f_1 = 8.81$  GHz,  $f_2 = 13.95$  GHz,  $Q_1 \simeq 7340$ , and  $Q_2 \simeq 4650$ . Fig. 3b shows a good agreement between the expected cavity photon rate and the experiment. From this data, we verify that only the first two modes contribute to the detector response at these temperatures, while the higher frequency modes are irrelevant. The detection efficiency  $\eta_2$  is as high as 40% for the mode  $f_2$ , with a dark count rate of 0.1 Hz. In this experiment, the estimated efficiency is a convolution between the antenna coupling and the detector efficiency, and is therefore a lower limit. For instance,  $\eta_1 \simeq 1\%$  is mainly due to the weak coupling of the antenna to the

mode  $f_1$ , as can be deduced from Fig. 2b, as well as SPD coplanar antenna selectivity, aimed to efficiently receive 14 GHz photons. The choice of the antennas' couplings is tailored to swap the main contribution to  $r_c(T)$  from  $f_1$  to  $f_2$  at a temperature of about 50 mK, therefore forming a peculiar cavity response within the dynamics of the detector, as shown in Fig. 3b.

Since a signature of single mode thermal photons is their super-Poissonian statistics [18], let us study the ratio of the SPD mean switching time  $\tau$  to its standard deviation  $\sigma$ . It is known that in the case of Poissonian statistics, which is a natural statistics of thermal or quantum dark counts of our detector, this ratio should be equal to unity [58]. In Fig. 3c the  $\tau/\sigma$  ratio vs temperature is shown. One can see that at low and high temperatures  $\tau/\sigma$  is close to unity, proving the Poissonian statistics of photons. At intermediate temperatures,  $\tau/\sigma$  is significantly lower than unity, reaching the minimum value of 0.73 at 47 mK. This is the evidence of the super-Poissonian distribution of photons, also referred to as photon bunching. Fig. 4 illustrates how it is reflected in the probability density distributions.

The time intervals between the events are presented as switching time distributions in Fig. 4 and fitted with an exponential distribution. This probability density for noise-induced escapes (or tunneling) across (through) the barrier should represent Poissonian distribution in the form  $w(t) = \exp(-t/\tau)/\tau$  [58]. One can see that the curve for 21 mK is fitted by the above exponential dependence without any fitting parameter for  $\tau = 9.026$  s. The curve for 80 mK is also well-fitted by exponential dependence with  $\tau = 7.214$  ms. In all cases,  $\tau$  is taken directly from the experimental data as the mean time interval between the events. At the same time, at 47 mK, the switching time distribution is better fitted by the power dependence  $t^{-\alpha}$  with  $\alpha = 0.75$  than by exponential dependence with  $\tau = 0.119$  s, at least for intermediate switching times. This is the evidence of quantum chaos [21] as natural statistics of thermal photons [18], and is further discussed in the Methods. The change from Poissonian distribution at low temperatures to super-Poissonian at intermediate and back to Poissonian at high temperatures can be explained in the following way. At low temperatures, when the thermal photons in the cavity are very rare, the Poissonian statistics is the internal statistics of the detector as, e.g., for noise-induced escapes across a potential barrier [58]. With temperature increase, the contribution of thermal photons from a single 8.81 GHz mode starts to dominate, that, as argued in [18], should demonstrate the super-Poissonian statistics (see the mode contribution vs temperature in Fig. 3b). With further increase of the temperature, the main 14 GHz mode starts to compete with the first one (their contributions become equal at 56 mK), that leads to Poissonization of the thermal photon statistics, according to [18]. To our knowledge, this is the first obser-

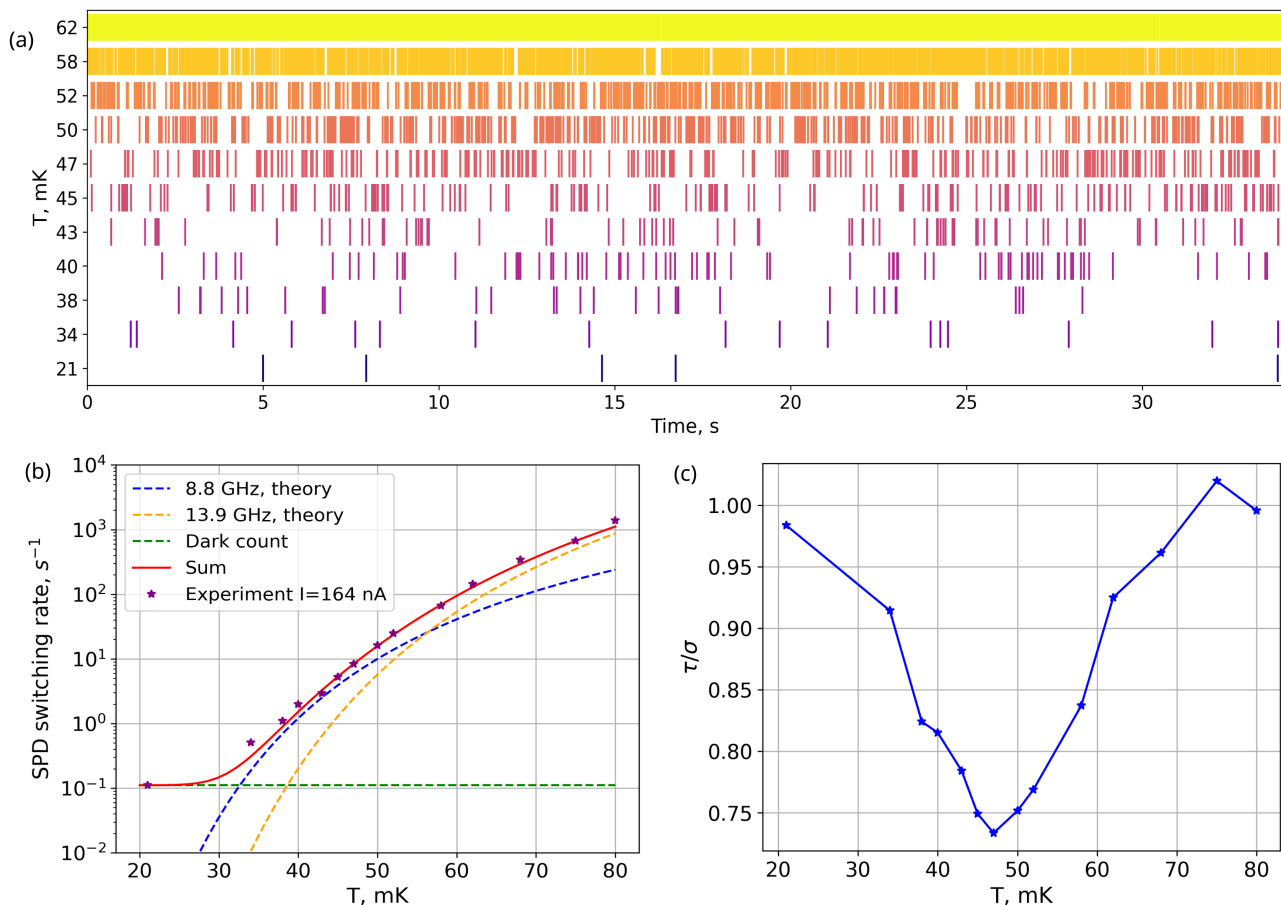


FIG. 3. Single microwave photon detection. a) An event plot of the recorded data is shown at various temperatures. b) The SPD switching rate, fitted with the theoretical photon rate, using formula (1). The error bars do not exceed the dot sizes. The data are fitted with the expected cavity photon rate  $r_c$  (1) plus a dark count rate  $r_{DC}$  to extract the efficiency and noise floor of the detector. The values of quantum efficiency  $\eta$  reach 0.0125 and 0.4 for 8.81 GHz and 13.9 GHz modes, respectively. c) The  $\tau$  to  $\sigma$  ratio vs cavity temperature, showing deviation from Poissonian statistics.

vation of super-Poissonian statistics of microwave thermal photons.

In this work we describe and operate a microwave single photon detector used to observe the ticking and the statistics of thermal photons emitted by a resonator at ultracryogenic temperatures. The Josephson junction-based sensor shows sub-Hz dark count rate and high efficiency, combined with a reduced operation complexity compared to qubit-based designs [9, 43]. The SPD was used to observe single microwave photons emitted by a single-mode and multi-mode thermal source, i.e. a copper cavity. Although widely accepted [18, 59, 60], an experimental demonstration of the super-Poissonian statistics of thermal microwave photons was, to our knowledge, missing. The measured photon rate is consistent with thermal emission from the microwave cavity modes, and closely follows the expected temperature dependence. The photon distribution displays a clear reduction of the mean to standard deviation ratio when

the light is emitted mainly by one mode, which instead remains unitary for dark count and multi-mode emission. The dynamical range of the detector extends from its dark count rate to the kHz range and is currently limited by the acquisition electronics' speed. The detector dynamics was not further investigated, and will be the subject of future works. The SPD efficiency can be better characterised with an on-demand microwave photon source [61, 62], to disentangle it from other systematic uncertainties. Future efforts to improve the SPD aim mainly at improving its dark count rate. For instance, a junction with lower  $I_C$  could enter the phase diffusion regime, which is expected to increase its lifetime, and thereby reduce the dark count rate [17]. Advancing the screening and filtering of the setup is also foreseen to improve the detector performances. In perspective, this work paves the way to a deeper examination of thermal light's quantum properties, and to their use to study quantum chaos [21], ghost imaging [63–65], and more

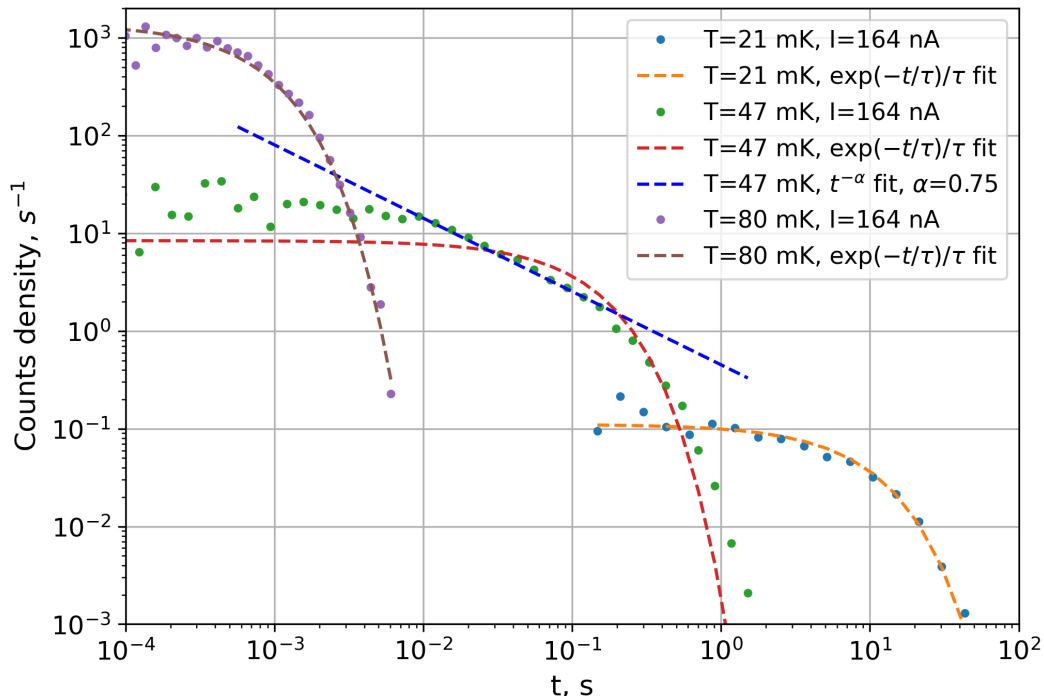


FIG. 4. Distribution of times between sequential switchings of the SPD at three various temperatures. The experimental data (dots) are fitted by  $\exp(-t/\tau)/\tau$  (dashed curves) without any fitting parameters with the mean switching time  $\tau$  directly taken from experimental data. Good agreement between fitting and experiment is observed at 21 mK and 80 mK cavity temperatures. One can note super-Poissonian distribution at intermediate cavity temperature 47 mK.

[18]. The device itself finds numerous applications in the field of precision physics beyond the Standard Model, as for instance Axion searches [22, 51]. On one hand, the performance requirements needed to drastically improve current Axion experiments are already met by the current device, on the other hand, these apparatus typically include strong magnetic field and long operation times, posing a challenge to the screening and long-term-stability of the detector. Nevertheless, the implementation of single microwave photon detectors such as the one presented here fosters the emergence of next-generation beyond the Standard Model experiments.

#### ACKNOWLEDGMENTS

The work is supported by the Russian Science Foundation (Project No. 19-79-10170). This project is also supported by the Italian Institute of Nuclear Physics (INFN) within the QUAX experiment. The authors wish to thank G. Carugno for triggering the interest on photon detectors and for the multiple advice in the course of this work, A.A. Yablokov for writing automated Python-based software, and I.V. Rakut' for sample holder fabrication.

#### AUTHOR CONTRIBUTIONS

The general idea of the work was suggested by L.S.K., N.C., A.V.G. and A.L.P. The sample fabrication was performed by A.V.G and A.V.B. A.L.P. ran the experiment with support of A.V.G., A.V.C. and L.S.R. Data were analyzed by N.C., A.L.P., A.V.G. and A.V.C. A.L.P., A.V.G., L.S.R. and A.V.B. designed and assembled the experiment. The cavity was designed by N.C., and tested by N.C., A.L.P., A.V.G. and A.V.C. All authors, led by N.C. and A.L.P., contributed to the manuscript with figures created by N.C., A.V.G. and A.V.C.

\* alp@ipmras.ru

† a.gordeeva@nntu.ru

- [1] C. M. Natarajan, M. G. Tanner, and R. H. Hadfield, *Superconductor Science and Technology* **25**, 063001 (2012).
- [2] E. D. Walsh, W. Jung, G.-H. Lee, D. K. Efetov, B.-I. Wu, K.-F. Huang, T. A. Ohki, T. Taniguchi, K. Watanabe, P. Kim, D. Englund, and K. C. Fong, *Science* **372**, 409 (2021).
- [3] K. Kouwenhoven, D. Fan, E. Biancalani, S. A. de Rooij, T. Karim, C. S. Smith, V. Murugesan, D. J. Thoen, J. J. Baselmans, and P. J. de Visser, *Phys. Rev. Appl.* **19**, 034007 (2023).

- [4] O. Astafiev, S. Komiyama, T. Kutsuwa, V. Antonov, Y. Kawaguchi, and K. Hirakawa, *Applied Physics Letters* **80**, 4250 (2002).
- [5] B. R. Johnson, M. D. Reed, A. A. Houck, D. I. Schuster, L. S. Bishop, E. Ginossar, J. M. Gambetta, L. DiCarlo, L. Frunzio, S. M. Girvin, and R. J. Schoelkopf, *Nature Physics* **6**, 663 (2010).
- [6] K. Inomata, Z. Lin, K. Koshino, W. D. Oliver, J.-S. Tsai, T. Yamamoto, and Y. Nakamura, *Nature Communications* **7**, 1 (2016).
- [7] S. Kono, K. Koshino, Y. Tabuchi, A. Noguchi, and Y. Nakamura, *Nature Physics* **14**, 546 (2018).
- [8] R. Lescanne, S. Deléglise, E. Albertinale, U. Réglade, T. Capelle, E. Ivanov, T. Jacqmin, Z. Leghtas, and E. Flurin, *Physical Review X* **10**, 021038 (2020).
- [9] E. Albertinale, L. Balembois, E. Billaud, V. Ranjan, D. Flanigan, T. Schenkel, D. Estève, D. Vion, P. Bertet, and E. Flurin, *Nature* **600**, 434 (2021).
- [10] J.-C. Besse, S. Gasparinetti, M. C. Collodo, T. Walter, P. Kurpiers, M. Pechal, C. Eichler, and A. Wallraff, *Physical Review X* **8**, 021003 (2018).
- [11] G. Oelsner, L. S. Revin, E. Il'ichev, A. L. Pankratov, H.-G. Meyer, L. Grönberg, J. Hassel, and L. S. Kuzmin, *Applied Physics Letters* **103**, 142605 (2013).
- [12] G. Oelsner, C. K. Andersen, M. Reháč, M. Schmelz, S. Anders, M. Grajcar, U. Hübner, K. Mølmer, and E. Il'ichev, *Physical Review Applied* **7**, 014012 (2017).
- [13] Y.-F. Chen, D. Hover, S. Sendelbach, L. Maurer, S. T. Merkel, E. J. Pritchett, F. K. Wilhelm, and R. McDermott, *Physical Review Letters* **107**, 217401 (2011).
- [14] A. Poudel, R. McDermott, and M. G. Vavilov, *Physical Review B* **86**, 174506 (2012).
- [15] L. S. Kuzmin, A. S. Sobolev, C. Gatti, D. Di Gioacchino, N. Crescini, A. Gordeeva, and E. Il'ichev, *IEEE Transactions on Applied Superconductivity* **28**, 2400505 (2018).
- [16] L. S. Revin, A. L. Pankratov, A. V. Gordeeva, A. A. Yablokov, I. V. Rakut, V. O. Zbrozhek, and L. S. Kuzmin, *Beilstein Journal of Nanotechnology* **11**, 960 (2020).
- [17] A. L. Pankratov, L. S. Revin, A. V. Gordeeva, A. A. Yablokov, L. S. Kuzmin, and E. V. Il'ichev, *npj Quantum Information* **8**, 1 (2022).
- [18] M. Fox, *Quantum Optics: An Introduction*, Oxford Master Series in Physics, Vol. 15 (Oxford University Press, 2006).
- [19] A. Kovalenko, D. Babjak, A. Lešundák, L. Podhora, L. Lachman, P. Obšil, T. Pham, O. Číp, R. Filip, and L. Slodička, *Optica* **10**, 456 (2023).
- [20] D. Bozyigit, C. Lang, L. Steffen, J. M. Fink, C. Eichler, M. Baur, R. Bianchetti, P. J. Leek, S. Filipp, M. P. da Silva, A. Blais, and A. Wallraff, *Nature Physics* **7**, 154 (2011).
- [21] I. I. Yusipov, O. S. Vershinina, S. V. Denisov, and I. M. V., *Chaos* **30**, ArticleSequenceNumber:023107 (2020).
- [22] S. K. Lamoreaux, K. A. van Bibber, K. W. Lehnert, and G. Carosi, *Phys. Rev. D* **88**, 035020 (2013).
- [23] G. Romero, J. J. García-Ripoll, and E. Solano, *Phys. Rev. Lett.* **102**, 173602 (2009).
- [24] L. C. G. Govia, E. J. Pritchett, C. Xu, B. L. T. Plourde, M. G. Vavilov, F. K. Wilhelm, and R. McDermott, *Phys. Rev. A* **90**, 062307 (2014).
- [25] A. Opremcak, I. V. Pechenezhskiy, C. Howington, B. G. Christensen, M. A. Beck, E. Leonard, J. Suttle, C. Wilen, K. N. Nesterov, G. J. Ribeill, T. Thorbeck, F. Schlenker, M. G. Vavilov, B. L. T. Plourde, and R. McDermott, *Science* **361**, 1239 (2018), <https://www.science.org/doi/pdf/10.1126/science.aat4625>.
- [26] A. L. Grimsmo, B. Royer, J. M. Kreikebaum, Y. Ye, K. O'Brien, I. Siddiqi, and A. Blais, *Physical Review Applied* **15**, 034074 (2021).
- [27] E. O. Göbel and U. Siegner, *The New International System of Units (SI) – Quantum Metrology and Quantum Standards*. (John Wiley & Sons, Ltd, 2019).
- [28] G. Brida, L. Ciavarella, I. P. Degiovanni, M. Genovese, L. Lolli, M. G. Mingolla, F. Piacentini, M. Rajteri, E. Taralli, and M. G. A. Paris, *New Journal of Physics* **14**, 085001 (2012).
- [29] J. Jaeckel and A. Ringwald, *Annual Review of Nuclear and Particle Science* **60**, 405 (2010), <https://doi.org/10.1146/annurev.nucl.012809.104433>.
- [30] R. J. Glauber, *Rev. Mod. Phys.* **78**, 1267 (2006).
- [31] M. Amenomori, Y. W. Bao, X. J. Bi, D. Chen, T. L. Chen, W. Y. Chen, X. Chen, Y. Chen, Cirennima, S. W. Cui, Danzengluobu, L. K. Ding, J. H. Fang, K. Fang, C. F. Feng, Z. Feng, Z. Y. Feng, Q. Gao, Q. B. Gou, Y. Q. Guo, H. H. He, Z. T. He, K. Hibino, N. Hotta, H. Hu, H. B. Hu, J. Huang, H. Y. Jia, L. Jiang, H. B. Jin, F. Kajino, K. Kasahara, Y. Katayose, C. Kato, S. Kato, K. Kawata, M. Kozai, Labaciren, G. M. Le, A. F. Li, H. J. Li, W. J. Li, Y. H. Lin, B. Liu, C. Liu, J. S. Liu, M. Y. Liu, Y.-Q. Lou, H. Lu, X. R. Meng, H. Mitsui, K. Munakata, Y. Nakamura, H. Nanjo, M. Nishizawa, M. Ohnishi, I. Ohta, S. Ozawa, X. L. Qian, X. B. Qu, T. Saito, M. Sakata, T. K. Sako, Y. Sengoku, J. Shao, M. Shibata, A. Shiomi, H. Sugimoto, M. Takita, Y. H. Tan, N. Tateyama, S. Torii, H. Tsuchiya, S. Udo, H. Wang, H. R. Wu, L. Xue, K. Yagisawa, Y. Yamamoto, Z. Yang, A. F. Yuan, L. M. Zhai, H. M. Zhang, J. L. Zhang, X. Zhang, X. Y. Zhang, Y. Zhang, Y. Zhang, Y. Zhang, Zhaxisangzhu, and X. X. Zhou (Tibet AS $\gamma$  Collaboration), *Phys. Rev. Lett.* **123**, 051101 (2019).
- [32] A. Bettini, *Introduction to elementary particle physics; 1st ed.* (Cambridge Univ. Press, Cambridge, 2008).
- [33] R. H. Hadfield, *Nature Photonics* **3**, 696 (2009), number: 12 Publisher: Nature Publishing Group.
- [34] I. Esmail Zadeh, J. Chang, J. W. N. Los, S. Gyger, A. W. Elshaari, S. Steinhauer, S. N. Dorenbos, and V. Zwiller, *Applied Physics Letters* **118**, 10.1063/5.0045990 (2021).
- [35] S. Khasminskaya, F. Pyatkov, K. Slowik, S. Ferrari, O. Kahl, V. Kovalyuk, P. Rath, A. Vetter, F. Hennrich, M. M. Kappes, G. Gol'tsman, A. Korneev, C. Rockstuhl, R. Krupke, and W. H. P. Pernice, *Nature Photonics* **10**, 727 (2016).
- [36] K. D. Irwin and G. C. Hilton, *Transition-Edge Sensors*, in *Cryogenic Particle Detection* (Springer, Berlin, Heidelberg, Germany, 2005) pp. 63–150.
- [37] S. Gleyzes, S. Kuhr, C. Guerlin, J. Bernu, S. Deléglise, U. Busk Hoff, M. Brune, J.-M. Raimond, and S. Haroche, *Nature* **446**, 297 (2007).
- [38] J. Govenius, R. E. Lake, K. Y. Tan, and M. Möttönen, *Physical Review Letters* **117**, 030802 (2016).
- [39] G.-H. Lee, D. K. Efetov, W. Jung, L. Ranzani, E. D. Walsh, T. A. Ohki, T. Taniguchi, K. Watanabe, P. Kim, D. Englund, and K. C. Fong, *Nature* **586**, 42 (2020).
- [40] R. Kokkoniemi, J.-P. Girard, D. Hazra, A. Laitinen, J. Govenius, R. E. Lake, I. Sallinen, V. Vesterinen, M. Partanen, J. Y. Tan, K. W. Chan, K. Y. Tan, P. Hako-

- nen, and M. Möttönen, *Nature* **586**, 47 (2020).
- [41] A. Blais, A. L. Grimsmo, S. M. Girvin, and A. Wallraff, *Reviews of Modern Physics* **93**, 025005 (2021).
- [42] B. Royer, A. L. Grimsmo, A. Choquette-Poitevin, and A. Blais, *Physical Review Letters* **120**, 203602 (2018).
- [43] A. V. Dixit, S. Chakram, K. He, A. Agrawal, R. K. Naik, D. I. Schuster, and A. Chou, *Physical Review Letters* **126**, 141302 (2021).
- [44] L. Balembois, J. Travesedo, L. Pallegoix, A. May, E. Billaud, M. Villiers, D. Estève, D. Vion, P. Bertet, and E. Flurin, *Phys. Rev. Appl.* **21**, 014043 (2024).
- [45] P. Sikivie, *Reviews of Modern Physics* **93**, 015004 (2021).
- [46] I. G. Irastorza and J. Redondo, *Progress in Particle and Nuclear Physics* **102**, 89 (2018).
- [47] T. Braine, R. Cervantes, N. Crisosto, N. Du, S. Kimes, L. J. Rosenberg, G. Rybka, J. Yang, D. Bowering, A. S. Chou, R. Khatiwada, A. Sonnenschein, W. Wester, G. Carosi, N. Woollett, L. D. Duffy, R. Bradley, C. Boutan, M. Jones, B. H. LaRoque, N. S. Oblath, M. S. Taubman, J. Clarke, A. Dove, A. Eddins, S. R. O’Kelley, S. Nawaz, I. Siddiqi, N. Stevenson, A. Agrawal, A. V. Dixit, J. R. Gleason, S. Jois, P. Sikivie, J. A. Solomon, N. S. Sullivan, D. B. Tanner, E. Lentz, E. J. Daw, J. H. Buckley, P. M. Harrington, E. A. Henriksen, and K. W. Murch (ADMX Collaboration), *Phys. Rev. Lett.* **124**, 101303 (2020).
- [48] O. Kwon, D. Lee, W. Chung, D. Ahn, H. Byun, F. Caspers, H. Choi, J. Choi, Y. Chong, H. Jeong, J. Jeong, J. E. Kim, J. Kim, C. Kutlu, J. Lee, M. Lee, S. Lee, A. Matlashov, S. Oh, S. Park, S. Uchaikin, S. Youn, and Y. K. Semertzidis, *Physical Review Letters* **126**, 191802 (2021).
- [49] C. M. Adair, K. Altenmüller, V. Anastassopoulos, S. Arguedas Cuendis, J. Baier, K. Barth, A. Belov, D. Bozicevic, H. Bräuninger, G. Cantatore, F. Caspers, J. F. Castel, S. A. Çetin, W. Chung, H. Choi, J. Choi, T. Dafni, M. Davenport, A. Dermenev, K. Desch, B. Döbrich, H. Fischer, W. Funk, J. Galan, A. Gardikiotis, S. Gninenko, J. Golm, M. D. Hasinoff, D. H. H. Hoffmann, D. Díez Ibáñez, I. G. Irastorza, K. Jakovčić, J. Kaminski, M. Karuza, C. Krieger, Ç. Kutlu, B. Lakić, J. M. Laurent, J. Lee, S. Lee, G. Luzón, C. Malbrunot, C. Margalejo, M. Maroudas, L. Miceli, H. Mirallas, L. Obis, A. Özbey, K. Özbozduman, M. J. Pivovarov, M. Rosu, J. Ruz, E. Ruiz-Chóliz, S. Schmidt, M. Schumann, Y. K. Semertzidis, S. K. Solanki, L. Stewart, I. Tsagris, T. Vafeiadis, J. K. Vogel, M. Vretenar, S. Youn, and K. Zioutas, *Nature Communications* **13**, 6180 (2022).
- [50] N. Crescini, D. Alesini, C. Braggio, G. Carugno, D. D’Agostino, D. Di Gioacchino, P. Falferi, U. Gambardella, C. Gatti, G. Iannone, C. Ligi, A. Lombardi, A. Ortolan, R. Pengo, G. Ruoso, and L. Taffarello, *Physical Review Letters* **124**, 171801 (2020).
- [51] R. Barbieri, C. Braggio, G. Carugno, C. S. Gallo, A. Lombardi, A. Ortolan, R. Pengo, G. Ruoso, and C. C. Speake, *Physics of the Dark Universe* **15**, 135 (2017).
- [52] K. M. Backes, D. A. Palken, S. A. Kenany, B. M. Brubaker, S. B. Cahn, A. Droster, G. C. Hilton, S. Ghosh, H. Jackson, S. K. Lamoreaux, A. F. Leder, K. W. Lehnert, S. M. Lewis, M. Malnou, R. H. Maruyama, N. M. Rapis, M. Simanovskaia, S. Singh, D. H. Speller, I. Urdinaran, L. R. Vale, E. C. van Assendelft, K. van Bibber, and H. Wang, *Nature* **590**, 238 (2021).
- [53] A. A. Clerk, M. H. Devoret, S. M. Girvin, F. Marquardt, and R. J. Schoelkopf, *Reviews of Modern Physics* **82**, 1155 (2010).
- [54] C. Braggio, L. Balembois, R. D. Vora, Z. Wang, G. Carugno, A. Ortolan, G. Ruoso, U. Gambardella, D. D’Agostino, P. Bertet, and E. Flurin, Quantum-enhanced sensing of axion dark matter with a transmon-based single microwave photon counter (2024), [arXiv:2403.02321 \[quant-ph\]](https://arxiv.org/abs/2403.02321).
- [55] A. Barone and G. Paternò, *Physics and applications of Josephson effect* (John Wiley & Sons, New York, 1982).
- [56] D. Pozar, *Microwave Engineering, 4th Edition* (Wiley, 2011).
- [57] O. Stanisavljević, J.-C. Philippe, J. Gabelli, M. Aprili, J. Estève, and J. Basset, Near-ideal microwave photon to electron conversion in a high impedance quantum circuit (2023), [arXiv:2312.14065 \[quant-ph\]](https://arxiv.org/abs/2312.14065).
- [58] A. N. Malakhov and A. L. Pankratov, Evolution Times of Probability Distributions and Averages — Exact Solutions of the Kramers’ Problem, in *Advances in Chemical Physics* (John Wiley & Sons, Ltd, Hoboken, NJ, USA, 2002) Chap. 6, pp. 357–438.
- [59] B. L. Morgan and L. Mandel, *Phys. Rev. Lett.* **16**, 1012 (1966).
- [60] F. Boitier, A. Godard, E. Rosencher, and C. Fabre, *Nature Physics* **5**, 267 (2009).
- [61] Z. H. Peng, S. E. de Graaf, J. S. Tsai, and O. V. Astafiev, *Nature Communications* **7**, 1 (2016).
- [62] Y. Zhou, Z. Peng, Y. Horiuchi, O. V. Astafiev, and J. S. Tsai, *Physical Review Applied* **13**, 034007 (2020).
- [63] A. Gatti, E. Brambilla, M. Bache, and L. A. Lugiato, *Phys. Rev. Lett.* **93**, 093602 (2004).
- [64] L.-H. Ou and L.-M. Kuang, *Journal of Physics B: Atomic, Molecular and Optical Physics* **40**, 1833 (2007).
- [65] Q. Liu, X.-H. Chen, K.-H. Luo, W. Wu, and L.-A. Wu, *Phys. Rev. A* **79**, 053844 (2009).